Research Article

Received: 2 April 2009 Revised: 29 April 2009 Accepted: 18 May 2009 Published online in Wiley Interscience: 17 September 2009

(www.interscience.wiley.com) DOI 10.1002/pi.2676

Kinetics and colloidal parameters of miniemulsion polymerization of butyl acrylate

Ufuk Yildiz,[a] Ignac Capek,[b]* Yanko Sarov,[c,d] Mihai C Corobea[e] and Julia Polovkova[b]

Abstract

BACKGROUND: The miniemulsion polymerization of butyl acrylate initiated by a macromonomeric azoinitiator (macroinimer, MIM) and stabilized by the non-ionic emulsifier Tween 60 (TW-60) was investigated.

RESULTS: The monomer conversion and the polymerization rate increase with the amount of MIM and then decrease. The desorption rate constants were estimated using the Ugelstad/O'Toole, Gilbert and Nomura models. The Ugelstad/O'Toole and Gilbert models suggest an increase in the k'_{des} value with increasing emulsifier concentration at the highest MIM concentration while the Nomura model proposes no variation in k'_{des} with an increase in both TW-60 and MIM concentrations. The polymerization rate increases in the following order with regard to initiator: MIM < ammonium persulfate < dibenzoyl peroxide < 2, 2′-azobisisobutyronitrile.

CONCLUSION: The increase in the rate of polymerization can be discussed in terms of both increased particle concentration and the gel effect. The size of the polymer particles decreases and the number of polymer particles increases with both TW-60 and MIM concentrations. This behaviour is attributed to the formation of a larger number of smaller monomer and/or polymer particles and higher particle nucleation rate. The observed long nucleation period for the MIM-initiated polymerization is attributed to the creation of a crosslinked structure and the immobilization of MIM chains.

Keywords: butyl acrylate; kinetics; macroinimer; macroinitiator; miniemulsion

INTRODUCTION

Macromonomeric initiators (macroinimers, MIMs), which behave as macromonomer, macroinitiator and macrocrosslinker, have attracted great interest because they allow the synthesis of crosslinked or branched block copolymers.[1–6] The polymerization of vinyl monomers with MIMs gives branched or crosslinked block copolymers depending on the MIM concentration and polymerization time.[7–12] A special feature of MIMs that are surface active is the incorporation of hydrophilic and initiator groups into the polymer matrix. The hydrophilic part of the MIM can be poly(ethylene oxide) (PEO). The PEO MIM in a polymerization acts as monomer, stabilizer and initiator. PEO-type MIMs impart stability to colloidal polymer particles.[13,14]

In previous papers, the dispersion polymerization of styrene and methyl methacrylate in the presence of MIMs[13,15] and the application of MIMs in microemulsion polymerization of styrene[16] were described. The effects of MIM type and concentration, polymerization time and temperature on the properties of dispersion and microemulsion polymerization were investigated. Miniemulsion polymerization is a way to synthesize polymer nanoparticles in the size range 50–500 nm with high morphological uniformity and chemical flexibility. Focusing on very small particles, miniemulsion polymerization already steps into the range of microemulsion polymerization, but with a minimum expense of surfactant which is up to a factor of 10 lower than in microemulsion formulations with similar particle size.[17] Miniemulsion polymerization has recently attracted much interest in terms of publications and the development of a wide range of useful polymer materials.[18–24] In contrast to conventional emulsion polymerization, in miniemulsion polymerization the monomer droplets become the predominant loci of particle nucleation. The total surface area of the droplets is such

* *Correspondence to: Ignac Capek, Slovak Academy of Sciences, Polymer Institute, Institute of Measurement Science, Dúbravská cesta 9, Bratislava, Slovakia. E-mail: upolign@savba.sk*

a *Kocaeli University, Department of Chemistry, 41380 Kocaeli, Turkey*

b *Slovak Academy of Sciences, Polymer Institute, Institute of Measurement Science, Dúbravská cesta 9, Bratislava, Slovakia*

c *MNES, IMNE, FEI, Technical University of Ilmenau, PF 100565, 98684 Ilmenau, Germany*

d *Central Laboratory of Optical Storage and Processing of Information, Bulgarian Academy of Sciences, PO Box 95, 1113 Sofia, Bulgaria*

e *National R-D Institute for Chemistry and Petrochemistry ICECHIM, Spl. Independentei 202, Bucharest, Romania*

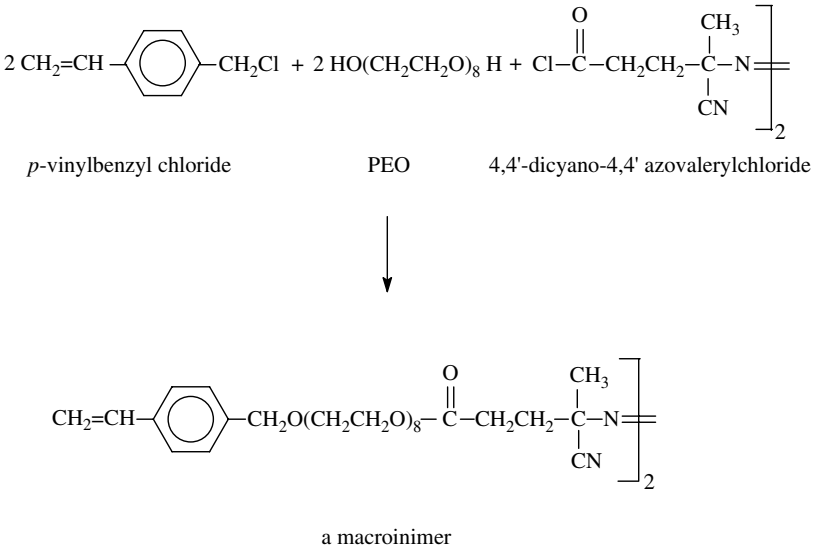

Scheme 1. Synthesis of a macroinimer.

that the surfactant is adsorbed predominantly on the droplets, which results in their unavailability to form micelles. The formation and stabilization of the droplets involve two steps in miniemulsion polymerization.

1. Pre-emulsification: preparation of a homogeneous mixture of monomer, surfactant, co-surfactant (or hydrophobe) and water.
2. Emulsification: homogenization of the monomer–water mixture, which under high shear breaks the droplets into nanometric sizes.

The droplets are consequently polymerized without changing their identity. Osmotic stability of the miniemulsion droplets results from osmotic pressure in the droplets, which balances the Laplace pressure and thus prevents monomer diffusion. The osmotic pressure results from the addition of the co-stabilizer, which has extremely low water solubility.[25] The colloidal stability of the miniemulsion droplet is achieved by the addition of a surfactant. The presence of a surfactant and a co-stabilizer (hydrophobe) prevents coalescence and Ostwald ripening. Coalescence (coagulation) is the process of the formation of a droplet from two or more smaller droplets, with the significant step occurring when the two droplets get close enough to allow contact of the droplet phases. In Ostwald ripening (molecular diffusion), large droplets grow at the expense of small ones, that is, the large becomes larger while small becomes smaller.

The object of the study reported here was to follow the miniemulsion kinetics and determine the kinetic parameters of the miniemulsion polymerization of butyl acrylate (BuA) initiated by MIM which can act as a macroinitiator and macrocrosslinker and also imparts colloidal stability to the polymer particles. This is the first attempt in the literature of this field dealing with the effect of MIM on the kinetic and colloidal parameters of the miniemulsion polymerization of BuA.

Due to the many results, the crosslink density and gelation properties of the polymers will be reported in later work to obtain useful and detailed information to understand the nature of the miniemulsion polymerization of BuA in the presence of MIM.

EXPERIMENTAL

Materials

Commercially available BuA was purified by distillation under reduced pressure before use. Commercially available polystyrene (Aldrich; M_w = 200 000 g mol^{-1}) was used as hydrophobe in the miniemulsion polymerization. Reagent-grade polyoxyethylene sorbitan monostearate (Tween 60, TW-60; Fluka) was used as emulsifier. Analytical-grade PEO, 4,4′-dicyano-4,4′-azovaleric acid and 4-vinylbenzyl chloride (Fluka) were used to synthesize PEO-based MIM according to the procedure described previously.[26] Ammonium persulfate (APS), 2,2′-azobisisobutyronitrile (AIBN) and dibenzoyl peroxide (DBP) (Aldrich) were used as supplied. Twice-distilled water was used as the polymerization medium.

Recipe and procedures

Miniemulsion polymerizations were carried out at 60 °C. The polymerization mixture consisted of 1.5 g of monomer (BuA), 15 g of continuous phase (water) and 0.015 g of polystyrene (hydrophobe). The amount of emulsifier (TW-60) and initiator (MIM) varied as detailed later. First a mixture of polystyrene in BuA was prepared. The mixture was stirred until the polystyrene was well dissolved in the monomer. After stirring, the emulsifier and water were added and then the monomer dispersion was homogenized (20 000 rpm; Ultra Turrax, IKA Works, USA) for 10 min at room temperature. After homogenization, MIM was added as the initiator of the polymerization. All the mixtures were bubbled with nitrogen gas to remove oxygen before starting the polymerization. The polymerization technique, determination of conversion, particle size measurements and estimation of polymerization rate were the same as described previously.[27–30] Polymer latexes were dialysed for *ca* two weeks against distilled water saturated with emulsifier.

Synthesis of MIM

A typical MIM can be synthesized by the reaction of 4,4′-dicyano-4,4′-azovaleryl chloride, PEO and 4-vinylbenzyl chloride (Scheme 1).

Characterization

The particle size of the latexes was analysed using dynamic light scattering with a model BI-90 particle sizer (Brookhaven Instruments Corp.).

Infrared spectroscopy was performed using a Nicolet 510 P FTIR instrument in the spectral range between 4000 and 400 cm^{-1}.

The molecular weights of the MIM were determined using gel permeation chromatography (GPC) analysis. GPC chromotograms were obtained using on a Shimadzu GPC instrument including a CR-4A chromotopac computer and printer, a CTO-6A column furnace, an RID-6A detector and an LC-9A liquid pump. Distilled tetrahydrofuran was used as eluent at a flow rate of 0.75 mL min^{-1}. Molecular weight and molecular weight distribution were calculated based on polystyrene standards. The molecular weight, M_w, of the MIM was determined using GPC as 10.2×10^2 g mol^{-1} ($M_w/M_n = 1.06$).

RESULTS AND DISCUSSION

Polymerization rate and kinetic parameters

MIM was prepared by the reaction of 4,4′-dicyano-4,4′-azovaleryl chloride, PEO and 4-vinylbenzyl chloride and used in the miniemulsion polymerization of BuA. The monomer conversion *versus* time curves of miniemulsion polymerization of BuA in the presence of MIM are shown in Figs 1 and 2. The polymerizations were carried out under the same conditions but with different concentrations of MIM (amounts varied from 0.0185 to 0.1515 g) and TW-60 (from 0.04 to 0.16 g). In all cases the curves are concave downward and have a typical sigmoidal shape. Initially, after a long nucleation period, the polymerization starts with high rate and after high conversions the rate gradually decreases. The total conversions (*ca* 90–100%) are reached at *ca* 60–80 min. However, the maximum conversion was 70% in the case of the highest MIM concentration. The conversion curves indicate that the length of the nucleation period is nearly inversely proportional to the MIM concentration. The longest nucleation periods of 25–35 min are observed in the runs with the highest MIM (0.1515 g) concentration (Fig. 1). For the lower MIM (0.075 g) concentration the nucleation period varies in the range 15–25 min. In the runs with amounts of MIM of 0.0375 and 0.0185 g nucleation periods are below 5 min (except one which can be attributed to the inhibition caused by oxygen; Fig. 2). These results indicate that MIM may also take part in homogeneous nucleation. The generated primary particles are adsorbed by monomer droplets. The final conversion of *ca* 70% (or very slow polymerization at this conversion) in the runs with 0.1515 g of MIM is in favour of polymerization in the continuous phase.

The monomer conversion at maximum polymerization rate (conv.$_{Rpmax}$) increases with the amount of MIM up to 0.0375 g of MIM, and then decreases. The conv.$_{Rpmax}$ also slightly increases with increasing concentration of emulsifier while the final monomer conversion (conv.$_f$) increases with the amount of emulsifier except for the system with the smallest MIM concentration (Fig. 3). In the case of the smallest MIM concentration, conv.$_f$ decreases in a complex way with increasing emulsifier concentration. The final conversions vary from *ca* 90 to 50% on varying the amount of MIM from 0.075 to 0.1515 g. The decrease in conversion (final or at R_{pmax}) with increasing MIM concentration can be reasonably ascribed to the formation of greater crosslinked polymer nanoparticles or microgels. A few swelling experiments were carried out with toluene and the results support the idea that a higher MIM concentration leads to lower swelling ratios due to greater crosslinking. Furthermore, we can also discuss the decrease in conversion in terms of the hairy layer around the particles on the decreased entry of initiating radicals, especially bulky PEO radicals, to the polymer particles as described by Guo *et al*.[31] The increased fraction of immobilized MIM in the crosslinked microgels is supposed to decrease the concentration of free or mobile radicals at high conversion conditions.

The conversion–time data for the miniemulsion polymerization of BuA initiated by MIM were used to estimate the rate of polymerization. This dependence is described by a curve with a maximum rate at a certain conversion (Figs 4 and 5). The maximum rates increase up to *ca* 30–50% conversion range at different MIM and TW-60 concentrations, and then decrease.

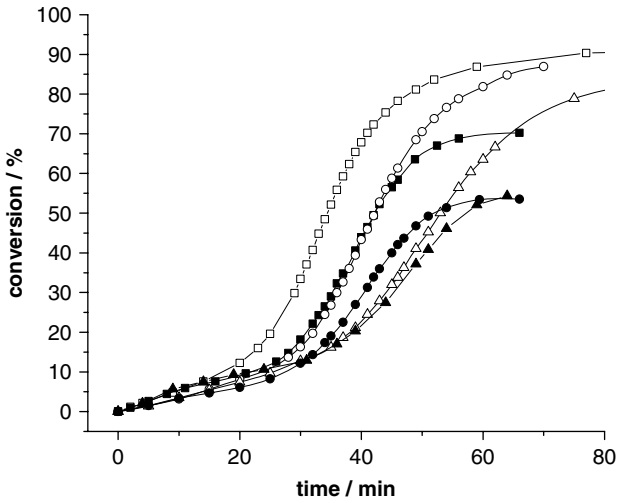

Figure 1. Variation of monomer conversion with reaction time and TW-60 and MIM concentrations in the miniemulsion polymerization of BuA (1.5 g BuA, 15 g water, 0.015 g polystyrene, MIM and TW-60): ■, 0.1515 g MIM and 0.16 g TW-60; ▲, 0.1515 g MIM and 0.08 g TW-60; ●, 0.1515 g MIM and 0.04 g TW-60; □, 0.075 g MIM and 0.16 g TW-60; ○, 0.075 g MIM and 0.08 g TW-60; △, 0.075 g MIM and 0.04 g TW-60.

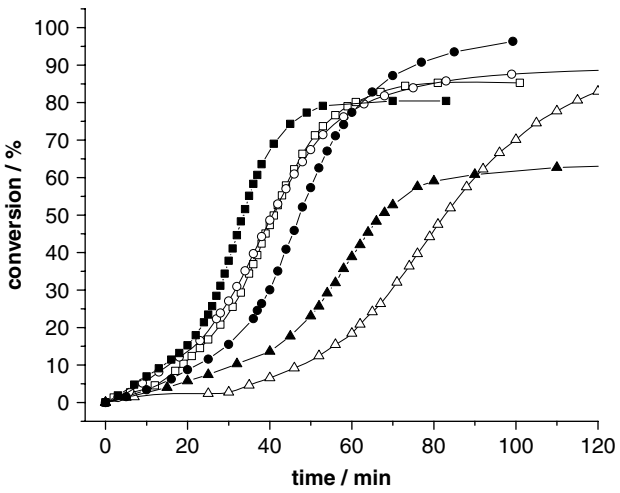

Figure 2. Variation of monomer conversion with reaction time and TW-60 and MIM concentrations in the miniemulsion polymerization of BuA (1.5 g BuA, 15 g water, 0.015 g polystyrene, MIM and TW-60): ■, 0.0375 g MIM and 0.16 g TW-60; ▲, 0.0375 g MIM and 0.08 g TW-60; ●, 0.0375 g MIM and 0.04 g TW-60; □, 0.0185 g MIM and 0.16 g TW-60; ○, 0.0185 g MIM and 0.08 g TW-60; △, 0.0185 g MIM and 0.04 g TW-60.

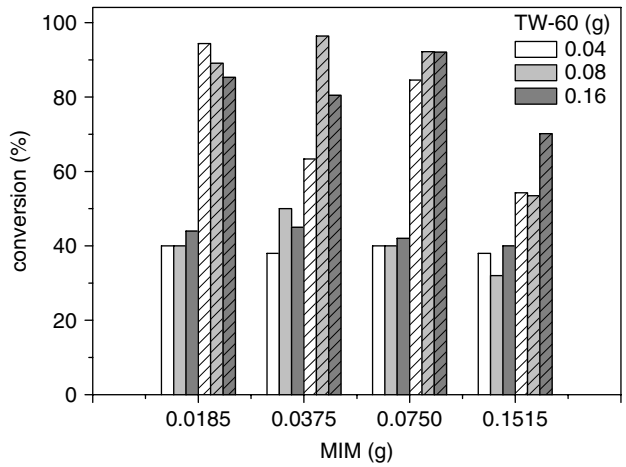

Figure 3. Variation of monomer conversion at maximum polymerization rate and the final monomer conversion (hatched bars) with the amount of MIM and TW-60 in the miniemulsion polymerization of BuA.

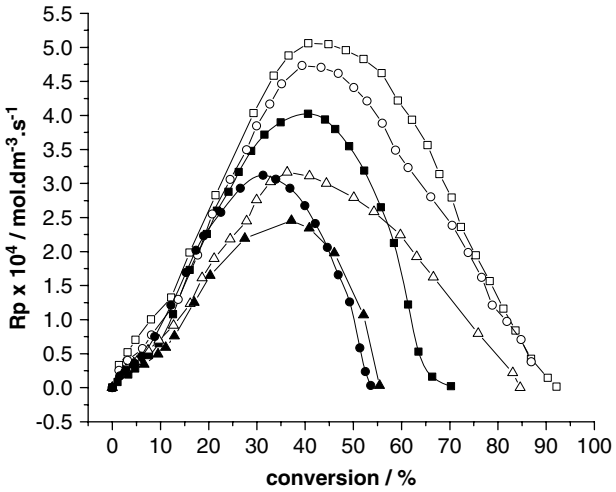

Figure 4. Dependence of polymerization rate on monomer conversion in the miniemulsion polymerization of BuA in the presence of MIM (1.5 g BuA, 15 g water, 0.015 g polystyrene, MIM and TW-60): ■, 0.1515 g MIM and 0.16 g TW-60; ▲, 0.1515 g MIM and 0.08 g TW-60; ●, 0.1515 g MIM and 0.04 g TW-60; □, 0.075 g MIM and 0.16 g TW-60; ○, 0.075 g MIM and 0.08 g TW-60; △, 0.075 g MIM and 0.04 g TW-60.

The pronounced increase in the rate of polymerization can be discussed in terms of both increased particle concentration and the gel effect. The gel effect of alkyl acrylates in bulk polymerization is known to be located at *ca* 20–30% conversion. The abrupt decrease in the polymerization rate beyond *ca* 30–50% conversion can be discussed in terms of the decrease in monomer concentration at the reaction loci and the immobilization of initiator due to the increased fraction of polymer gel with increasing MIM concentration. The formation of crosslinked nanostructures decreases the monomer concentration within the polymer particles at medium and high conversions. The results shown in Figs 4 and 5 and Table 1 show that the maximum rate of polymerization varies with conversion and MIM concentration in a complex way. The data summarized in Fig. 6 show that the dependence of the rate of polymerization on the MIM concentration for all TW-60 concentrations is described by a curve with a maximum at [MIM] = 0.075 g. The dependence of

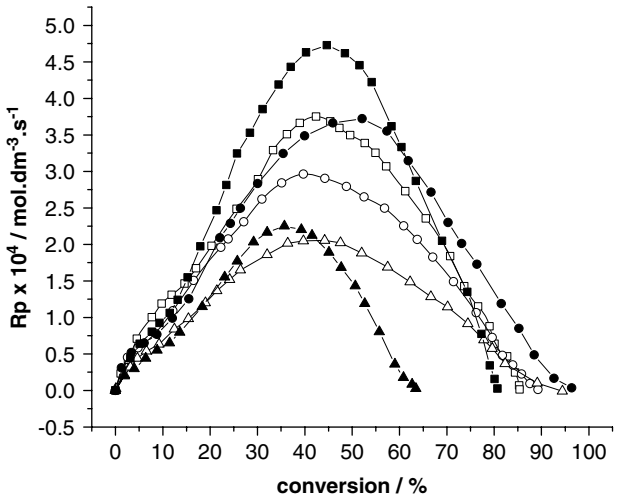

Figure 5. Dependence of polymerization rate on monomer conversion in the miniemulsion polymerization of BuA in the presence of MIM (1.5 g BuA, 15 g water, 0.015 g polystyrene, MIM and TW-60): ■, 0.0375 g MIM and 0.16 g TW-60; ▲, 0.0375 g MIM and 0.08 g TW-60; ●, 0.0375 g MIM and 0.04 g TW-60; □, 0.0185 g MIM and 0.16 g TW-60; ○, 0.0185 g MIM and 0.08 g TW-60; △, 0.0185 g MIM and 0.04 g TW-60.

log R_{pmax} *versus* log[MIM] was used to estimate the following reaction orders: $x_1 = 0.308$ for [TW-60] = 0.16 g, $x_2 = 0.335$ for [TW-60] = 0.08 g and $x_3 = 0.335$ for [TW-60] = 0.04 g, or

$$R_{pmax} \propto [MIM]^{x_1}; \quad R_{pmax} \propto [MIM]^{x_2}; \quad R_{pmax} \propto [MIM]^{x_3}$$

The reaction orders 0.31–0.33 are closer to the reaction order of 0.4 for the emulsion polymerization[32,33] than to the reaction order of 0.5 for the solution polymerization. This indicates that at conv.$_{Rpmax}$ (at medium conversions) the polymerization should be governed by the emulsion polymerization model. Thus, the increase in the polymerization rate with increasing MIM concentration can be attributed to the increased nucleation of polymer particles (or number of reaction loci). Above [MIM] = 0.075 g the rate of polymerization decreases due to the decrease in monomer concentration at the reaction loci and the immobilization of initiator. The maximum rate of the polymerization increases with TW-60 concentration with the following reaction orders: $y_1 = 0.434$ for [MIM] = 0.0185 g, $y_2 = 0.535$ for [MIM] = 0.0375 g, $y_3 = 0.339$ for [MIM] = 0.075 g and $y_4 = 0.356$ for [MIM] = 0.1515 g, or

$$R_{pmax} \propto [TW\text{-}60]^{y_1}; \quad R_{pmax} \propto [TW\text{-}60]^{y_2}; \quad R_{pmax} \propto [TW\text{-}60]^{y_3}; \quad R_{pmax} \propto [TW\text{-}60]^{y_4}$$

The increase in the polymerization rate with emulsifier (TW-60) can be attributed to the increased nucleation of polymer particles (number of reaction loci). The reaction orders vary in the range 0.34–0.54 and are somewhat smaller than 0.6 for the classic emulsion polymerization.[32,33] The contribution of increased density of surfactant layer on the particle surface decreases the entry rate of radicals. The reaction order also decreases with increasing MIM concentration. The increased MIM concentration increases the crosslinked density of polymer particles which favours both the exit rate of radicals from particles and the polymerization on the particle surface. The decrease in R_{pmax} thus

Table 1. Variation of kinetic and colloidal parameters with the surfactant concentration in the miniemulsion polymerization of BuA with conversion and MIM and TW-60 concentrations

MIM (g)	TW-60 (g)	$R_{pmax} \times 10^4$/conv.$_{Rpmax}$ (mol dm^3 s^{-1}/%)	$\overline{n}$ (particles)	d_d (nm)	d_p (nm) (a)	d_p (nm) (b)	N_d ($\times 10^{-16}$ dm^{-3})	N_p ($\times 10^{-16}$ dm^{-3}) (a)	N_p ($\times 10^{-16}$ dm^{-3}) (b)	N_p/N_d (a)	N_p/N_d (b)
–	0.04			140			7.1				
–	0.08			125			10.0				
–	0.16			110			15.0				
0.0185	0.040	2.054/40	0.192	250	178	155	1.2	1.2	4.8	1.0	4.0
0.0185	0.080	2.964/40	0.138	220	145	139	1.8	2.4	6.3	1.3	3.5
0.0185	0.160	3.750/44	0.113	180	129	119	3.3	3.7	9.7	1.1	3.0
0.0375	0.040	2.251/38	0.120	220	155	148	1.8	2.1	5.0	1.2	2.8
0.0375	0.080	3.722/50	0.095	211	130	114	2.1	4.4	11.4	2.1	5.4
0.0375	0.160	4.726/45	0.106	161	118	107	4.6	5.0	12.5	1.0	2.7
0.0750	0.040	3.163/40	0.098	205	132	119	2.2	3.6	9.6	1.6	4.4
0.0750	0.080	4.735/40	0.152	200	128	115	2.4	3.5	11.6	1.4	4.8
0.0750	0.160	5.059/42	0.098	140	110	104	7.1	5.8	15.6	0.8	2.0
0.1515	0.040	2.456/38	0.106	200	149	148	2.4	2.0	5.2	0.8	2.2
0.1515	0.080	3.121/32	0.145	180	132	123	3.3	2.6	8.1	0.8	2.4
0.1515	0.160	4.023/40	0.062	130	100	96	8.8	7.2	18.0	0.8	2.0

Reaction: 1.5 g BuA (0.78 mol dm^{-3} water), 15 g water, 0.015 g polystyrene.
(a) At conv.$_{Rpmax}$ (conversion at R_{pmax}); (b) at final conversion.
N_p, number of polymer particles; N_d, initial number of monomer droplets; N_p/N_d, ratio between number of polymer particles and initial number of monomer droplets.

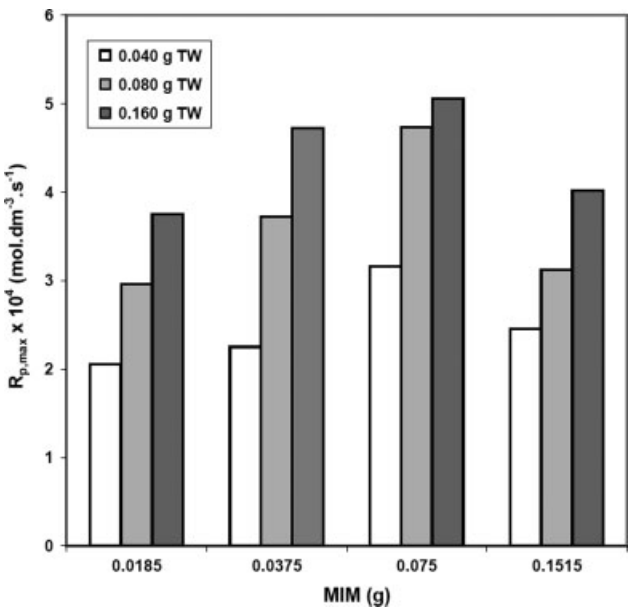

Figure 6. Variation of maximum polymerization rate with MIM and TW-60 concentrations in the miniemulsion polymerization of BuA.

can be discussed in terms of increased desorption of radicals from particles and increased polymerization at particle surfaces and in the aqueous phase. The calculated desorption rate constants and the number of radicals per particle ($\overline{n}$; Tables 1 and 2) confirm these ideas.

Kinetic and colloidal parameters

In radical polymerization it is well known that the rate of polymerization is given by the following quantitative theory of Harkins[32] and Smith–Ewart:[33]

$$R_p = k_p[M]_p \overline{n} N_p / N_A$$

where k_p is the propagation rate constant, $[M]_p$ the equilibrium monomer concentration in the polymer particles, $\overline{n}$ the average number of radicals per particle, N_p the number of particles per unit volume of the continuous (aqueous) phase and N_A the Avogadro constant.

The particle diameter (d_p), the number of polymer particles (N_p) and the average number of radicals per particle vary with surfactant and initiator concentration and conversion as shown in Table 1 and Figs 7 and 8. The size of the polymer particles decreases and the number of polymer particles increases with both the TW-60 and MIM concentration at conv.$_{Rpmax}$ and conv.$_f$. This is attributed to the formation of a greater number of smaller monomer and/or polymer particles and greater particle nucleation rate due to the surface active property of the MIM.

Table 1 presents the number of droplets (N_d) calculated from the diameters measured by light scattering. This table also includes the ratio between the number of polymer particles and the initial number of droplets (N_p/N_d). However, we are aware of some uncertainties associated with this ratio because an average diameter of the droplets was first estimated from the dynamic light scattering measurement and the third power of this value was used to estimate N_d. Furthermore, the stability of the monomer droplets was less than the stability of the polymer particles. Nevertheless, the values of N_p/N_d indicate some important trends. Most of the droplets are nucleated in runs with the highest MIM (01 515 g) concentration up to the conversion at R_{pmax}. A higher fraction of nucleated droplets found in these runs could be attributed to the higher stability of this miniemulsion. Indeed, it is observed that the addition of the smallest concentration of MIM leads to the formation of largest monomer droplets. For example, the addition of 0.0185 g of MIM to the run with 0.04 g of TW-60 leads to the

Table 2. Variation of desorption rate coefficients with TW-60 concentration in the miniemulsion polymerization of BuA at various amounts of MIM

MIM (g)	TW-60 (g)	a ($\times 10^4$)	m ($\times 10^2$)	k'_{des} ($\times 10^{11}$ cm^2 s^{-1})			k_{des} (s^{-1})			ρ_a (mol L^{-1} s^{-1})	ρ_a/ρ_i
		I	I	I	II	III	I	II	III	I	I
0.0185	0.040	37.62	13.197	0.84	11.0	0.774	4.07	5.596	0.394	1.27	2.60
0.0185	0.080	20.12	3.398	0.63	11.0	0.774	4.63	5.596	0.394	0.88	3.62
0.0185	0.160	3.16	3.598	0.52	11.0	0.756	4.78	7.347	0.505	0.70	4.42
0.0375	0.040	7.20	3.012	2.32	11.0	0.759	14.88	7.051	0.487	2.35	4.17
0.0375	0.080	6.75	1.016	1.33	11.0	0.746	12.07	8.359	0.568	1.42	5.26
0.0375	0.160	2.58	1.082	0.75	11.0	0.747	8.30	8.359	0.568	1.12	4.72
0.0750	0.040	9.98	2.635	3.12	11.0	0.690	27.53	14.644	0.919	3.36	5.10
0.0750	0.080	2.81	1.261	1.08	11.0	0.683	10.19	15.545	0.966	2.23	3.29
0.0750	0.160	1.85	0.649	1.34	11.0	0.683	17.09	15.545	0.966	2.08	5.10
0.1515	0.040	13.05	1.091	4.48	11.0	0.690	83.88	14.644	0.919	11.28	4.72
0.1515	0.080	3.53	0.671	3.52	11.0	0.825	31.06	0.972	0.073	6.34	3.45
0.1515	0.160	1.61	0.488	4.91	11.0	0.817	75.65	1.693	0.126	5.35	8.06

I, Ugelstad/O'Toole model; II, Nomura model; III, Gilbert model.

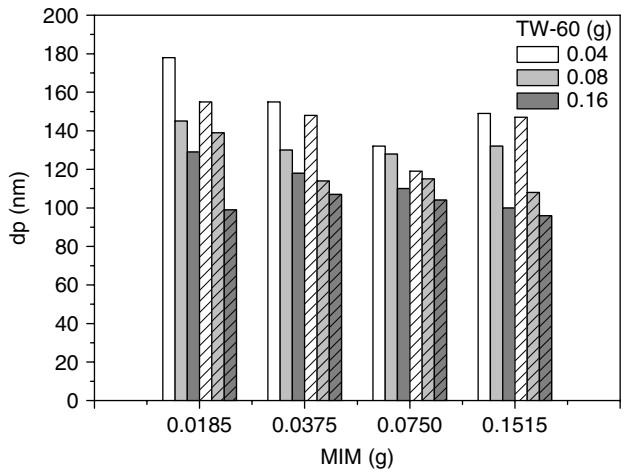

Figure 7. Variation of the diameter of poly(butyl acrylate) latex particles at maximum polymerization rate and final diameter (hatched bars) with MIM and TW-60 concentrations.

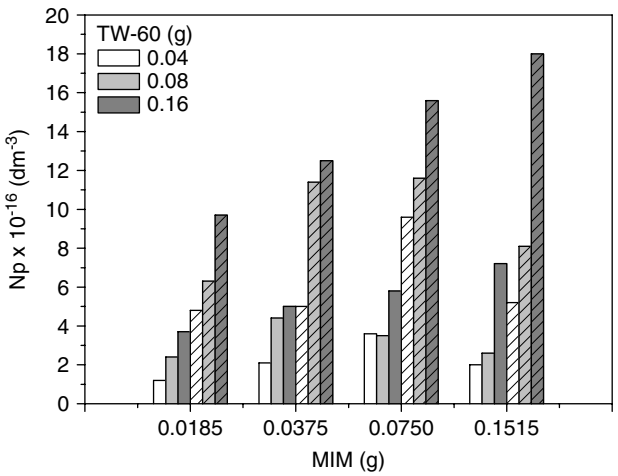

Figure 8. Variation of the number of final polymer particles at maximum polymerization rate and the number of final particles (hatched bars) per unit volume with MIM and TW-60 concentrations.

formation of monomer droplets with a diameter of *ca* 250 nm. On the contrary, the addition of 0.1515 g of MIM to the run with 0.16 g of TW-60 forms a dispersion with droplet diameter of *ca* 130 nm. Substantial secondary nucleation is observed in all runs but a secondary nucleation is inversely proportional to MIM concentration. Because there were no micelles in the system (the ratio N_p/N_d decreases with increasing emulsifier concentration), the particles are produced by homogeneous nucleation. These results show that the number of polymer particles is determined by the competition between droplet nucleation and homogeneous nucleation.[34] Droplet nucleation is strongly affected by the colloidal stability of miniemulsion droplets. Therefore, the lower droplet stability and large number of droplets are the likely reason for the high N_p/N_d ratio for MIM-initiated polymerization systems.

The probability of formation new particles increases as the number of particles/droplets in the system decreases.[34,35] The reason is that the oligomers in the aqueous phase can grow to a critical size for precipitation before being captured by the particles/droplets. This is what happened in run, whereas the number of droplets/particles in runs was high enough to minimize the occurrence of homogeneous nucleation.

The variation of the diameter of polymer particles and the number of polymer particles with monomer conversion for the two different recipes is shown at Figs 9 and 10. The diameter of the polymer particles decreases while the number of polymer particles increases with increasing monomer conversion. The decrease in the particle diameter with conversion can be discussed in terms of the continuous shrinkage of active monomer/polymer particles and the secondary particle nucleation. The shrinkage of active monomer/polymer particles is due to the initiation of polymerization and growth of polymer chains in monomer droplets. The formation of smaller particles with increasing conversion can also be attributed to the partial transfer of monomer from monomer droplets to active particles. The particle size of polymer particles is observed to decrease slightly after dialysis which indicates the presence of monomer in polymer particles. Furthermore the decrease in the average particle size is more pronounced for particles formed at low conversions. That is,

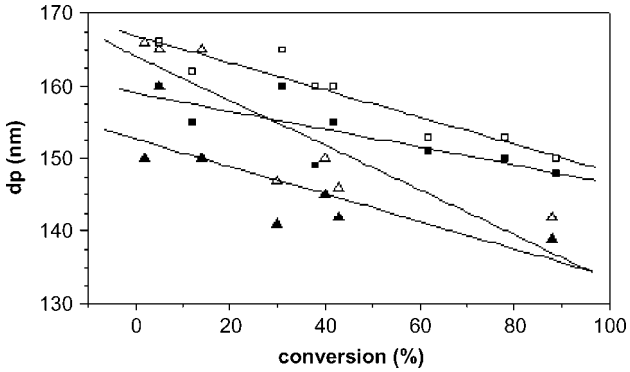

Figure 9. Variation of the diameter of poly(butyl acrylate) latex particles with monomer conversion in the presence of MIM (1.5 g BuA, 15 g water, 0.015 g polystyrene, MIM and TW-60); □, 0.1515 g MIM, 0.04 g TW-60, monomer saturated; ■, 0.1515 g MIM, 0.04 g TW-60, after dialysis; △, 0.0185 g MIM and 0.080 g TW-60, monomer saturated; ▲, 0.0185 g MIM and 0.080 g TW-60, after dialysis.

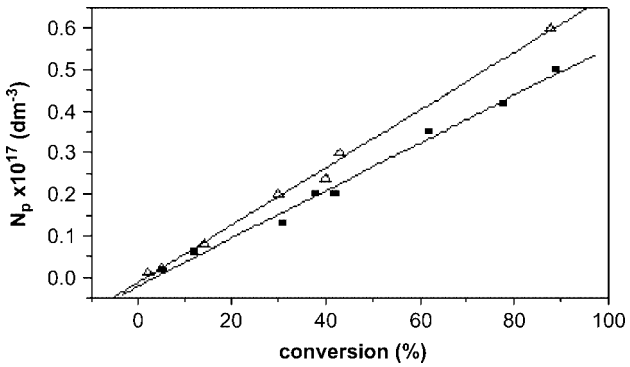

Figure 10. Variation of the number of final polymer particles per unit volume with monomer conversion in the presence of MIM (1.5 g BuA, 15 g water, 0.015 g polystyrene, MIM and TW-60): ■, 0.1515 g MIM, 0.04 g TW-60; △, 0.0185 g MIM, 0.080 g TW-60.

the concentration of monomer in latex particles is higher at low conversions than at high conversions.

The number of radicals per particle ($\bar{n}$) is much lower than 0.5 which indicates that desorption of radicals from polymer particles influences the polymerization process. The average number of radicals in a particle ($\bar{n}$) decreases with increasing both the MIM and TW-60 concentrations (Table 1). This indicates that the exit of monomeric radicals from particles increases with decreasing particle size and increased crosslinked density of polymer particles. The exit (desorption) rate constants k'_{des} ($cm^2\ s^{-1}$) and k_{des} (s^{-1}) were calculated to obtain more information about the radical exit events with three different models: the Ugelstad/O'Toole approach (I), the Nomura model (II) and the Gilbert model (III), as described in our previous paper.[36] The Ugelstad/O'Toole, Nomura and Gilbert models were directly applied to miniemulsion polymerization of BuA. The calculated exit rate constants for the miniemulsion polymerization of BuA are given in Table 2. The kinetic parameters used to estimate desorption rate constants k'_{des} ($cm^2\ s^{-1}$) and k_{des} (s^{-1}) for the miniemulsion polymerization of BuA are collected in Table 3. The initiator decomposition rate constant k_d for MIM was approximated with the k_d of PEGA initiator which has almost the same structure as MIM.[37]

According to the Ugelstad/O'Toole and Gilbert models the k'_{des} values decrease with increasing concentration of surfactant while

Table 3. Kinetic parameters for miniemulsion polymerization of BuA

Parameter	Numerical value
$k_{d,DBP}$	$2.83 \times 10^{-6}\ s^{-1}$
$k_{d,LPO}$	$1.42 \times 10^{-5}\ s^{-1}$
$k_{d,APS}$	$6.06 \times 10^{16} \times (-140\,167/RT)\ s^{-1}$
$k_{d,PEGA}$	$4.08 \times 10^{-6}\ s^{-1}$ at 60 °C
k_p	$7.37 \times 10^5 \times \exp(-1157/T)\ L\ mol^{-1}\ s^{-1}$
k_t (50 °C)	$17.13 \times 10^9 \times \exp(-1083/T)\ L\ mol^{-1}\ s^{-1}$
k_{fm} (50 °C) = k_{tr}	$2.9 \times 10^5 \times \exp(-3921/T)\ L\ mol^{-1}\ s^{-1}$
m_d	1/1050
M_p	2.35 mol dm^{-3}
D_w	$1.7 \times 10^{-5}\ cm^2\ s^{-1}$
D_c	$4.1 \times 10^{-5}\ cm^2\ s^{-1}$
D_p	$8.66 \times 10^{-7}\ cm^2\ s^{-1}$
C_w	6.4×10^{-3} mol dm^{-3}

the Nomura model proposes no variation in k'_{des} with increasing both TW-60 and MIM concentrations. The decrease is consistent with the concept that the densely packed emulsifier molecules make a barrier for the entering or exiting radicals. On the other hand, k'_{des} values do not follow a similar trend at the highest MIM concentration. This deviation can be discussed in terms of the advanced crosslinking and/or increased immobilization of MIM within the crosslinked polymer particles that affects the desorption of radicals in a complex way. The different trend in the k'_{des} values dependent on [MIM] is observed for both Ugelstad/O'Toole and Gilbert models by keeping surfactant concentration constant. The first model estimates an increase in the k'_{des} values (0.84, 2.32, 3.12 and 4.48 at constant amount of TW-60 of 0.04 g) with increasing [MIM]. The Gilbert model, in contrast, suggests a slight decrease in the values (0.77, 0.76, 0.69 and 0.69 at the same TW-60 concentration of 0.04 g). The difference can be ascribed to the different approaches in the evaluation of the k_{des} desorption rate constant which is dependent on the particle size. In the more simple Gilbert model, the k_{des} values vary only with the particle size. Indeed, when we follow the trend in the diameter of polymer particles with the MIM concentration (Fig. 7), we can see the slight decrease of the particle size with the amount of MIM up to 0.075 g of MIM. The same trend is found for the k_{des} values evaluated by the Gilbert model. The Ugelstad/O'Toole model also takes into account the re-absorption of desorbed radicals by the particles. In the model, the parameters a and m (Table 2) related to the adsorption of free radicals by polymer particles and desorption of radicals out of the particles, respectively, are used to calculate k_{des} values by an iterative approach comparing the experimental and theoretical number of radicals per particle. The adsorption of the radicals depends on the particle size and number of particles as well, while the desorption is mainly dependent on the particle size. The increase of the number of particles and decrease of the particle size with [MIM] result in the decrease of a ($a \approx d_p{}^3/N_p$).[36] On the other hand, the average number of radicals per particle ($\bar{n}$) with increasing amount of MIM generally decreases. If $a \ll m$, ($\bar{n}$) $\approx a/m$ and $m \approx k_{des}$[36] then to retain a decreasing trend of ($\bar{n}$), the decrease of m must be more moderate than the decrease of a, resulting finally in the increasing values of k_{des}. A greater amount of MIM increases the desorption rate constant of radicals. which is consistent with the experimentally obtained decrease of the average number of radicals per particle with increasing MIM concentration.

The increasing MIM concentration also increases the radical entry rate (ρ_a) and the ratio ρ_a/ρ_i. The increase in ρ_a with [MIM] can be discussed in terms of increased incorporation of the MIM-based radicals at particle surfaces or within particle shells. The MIM-*g*-PBuA oligomers are supposed to act as surface-active compounds which associate into aggregates and/or adsorb at particle surfaces which increases both the radical concentration and the colloidal stability of the polymer particles.

Variation of initiators

The MIM and its behaviour as sole surfactant and initiator and also as additional surfactant and initiator in the presence and absence of another initiator and surfactant in the miniemulsion polymerization of styrene has already been published.[38] In the present study, three types of initiators, APS, AIBN and DBP, were used to investigate the effect of the type of initiator and the high initiator concentration on the kinetics of the miniemulsion polymerization of BuA. The conversion–time curves for the miniemulsion polymerization of BuA initiated by various initiators are shown in Fig. 11. In the case of water-soluble initiator (APS) the conversion (conv.$_f$) reached the highest value (98%) in comparison with other initiators (Table 4). In this case the initiation is a two-step process. In the first step, the initiating radicals are formed by the decomposition of APS in the aqueous phase. Then, the hydrophilic primary radicals grow by propagation of BuA monomer dissolved in water. In the second step, the oligomeric radicals enter the monomer-swollen micelles or monomer-swollen polymer particles. The results show that the initiator efficiency is the highest for the APS system. In the reaction system with AIBN the radicals are formed in both the aqueous and monomer phases. DBP is supposed to generate primary radicals in the monomer phase. The amphiphilic MIM initiator or/and its graft oligomers are supposed to be located mostly at the particle interfaces or within the monomer-swollen micelles due to its hydrophilic and hydrophobic segments. Figure 11 shows that the shapes of the conversion curves for APS, AIBN and DBP differ from that of MIM. In the case of APS, AIBN and DBP, the polymerization is very fast from the start of polymerization, that is, the conversion curve is without a nucleation period. The MIM-initiated polymerization shows a conversion curve with a sigmoidal shape. The low polymerization rate up to *ca* 30% conversion can be attributed to both the slow (homogeneous) polymerization in the aqueous phase and the low entry rate of MIM radicals into the monomer droplets and polymer particles, that is, the MIM-derived radicals might experience a barrier on entering into particles due to both the high hydrophilic nature and bulky size of MIM-derived radicals. The fast MIM-initiated polymerization at medium conversions can be attributed to the increased number of particles, the re-entry of monomeric radicals into monomer droplets (second-order loss kinetics) and the gel effect. The monomer-transferred radicals do not find any barrier in their entry or exit history at medium conversions. Polymerizations initiated by APS, AIBN and DBP reach conversion in the range 83–98%. In contrast, the MIM-initiated polymerization achieves the lowest conversion (only 70%). The decrease or depletion of hydrophobic monomer (BuA) from the aqueous phase depresses the copolymerization of MIM radicals with monomer and the formation of more hydrophobic (surface-active) oligomeric radicals. The entry rate of such hydrophilic MIM radicals is depressed and hence so is the rate of polymerization.

Table 4 and Fig. 12 show that the polymerization rate increases in the following order: MIM < APS < DBP < AIBN. However, the molar concentration of initiator increases in the following order: MIM < DBP < APS < AIBN. These data indicate that APS and DBP do not follow the initiator concentration trend. In order to follow this deviation we estimated the fractional rates of polymerization $R_{p,f}$ (R_{pmax} divided by the initiator concentration) and its dependence on the type of initiator (Table 4).

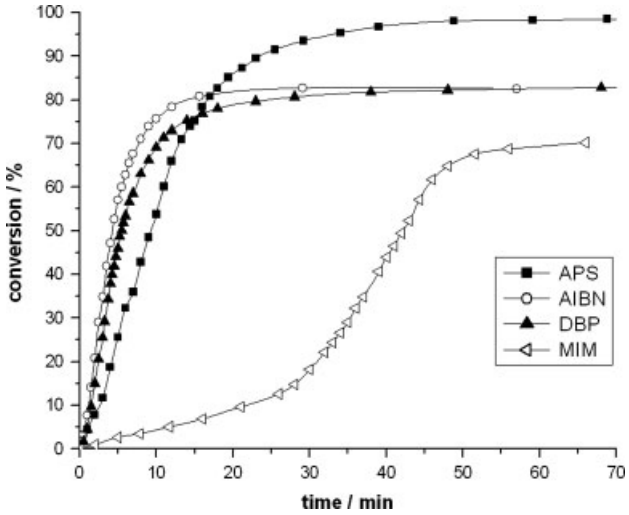

Figure 11. Variation of monomer conversion with reaction time in the miniemulsion polymerization of BuA initiated by various initiators (1.5 g BuA, 15 g water, 0.015 g polystyrene, 0.160 g TW-60, 0.1515 g initiator).

According to the micellar model (reaction order 0.4) the fractional rates (x) vary as follows: 0.25 (MIM) < 0.32 (APS) < 0.58 (DBP) < 0.61 (AIBN). The emulsion and microemulsion polymerizations of BuA initiated by the water-soluble initiator (APS) are faster than those initiated by the oil-soluble initiators (AIBN, DBP).[39] These data indicate that the polymerizations proceeding under a very high initiator concentration deviate from the general trend. This deviation can be discussed in terms of deactivation of both primary radicals derived from APS and desorbed monomeric radicals from polymer particles. Thus, the radical entry rate efficiency is strongly depressed. On the contrary, the deactivation of radicals is lower for the AIBN- or DBP-initiated polymerization. The use of an oil-soluble initiator such as DBP offers some potential advantages over conventional water-soluble initiators. DBP forms a pair of primary radicals in the oil phase (monomer droplets), polymerization loci, so the droplets need not capture a radical to be initiated. In the case of a partly water-soluble initiator, such as AIBN, single radicals are also formed in the aqueous phase from the fraction of oil-soluble initiator dissolved in water.

A terminal model (reaction order 0.5) suggests a similar trend: 0.4 (MIM) ≈ 0.43 (APS) < 0.8 (DBP) ≈ 0.81 (AIBN). A bimolecular termination of growing radicals is more pronounced in the systems with a water-soluble initiator. This can be discussed in terms of the bimolecular termination or primary radical termination at the particle surface and in the aqueous phase. The living nature of polymerization modelled in DBP and AIBN can be favoured by the immobilization (entanglement) of growing radicals in the crosslinked particle matrix.

A monomolecular termination approach (reaction order 1.0) suggests an increased rate for all initiators especially for MIM and DBP: 2.0 (APS) < 3.2 (AIBN) < 4.0 (DBP and MIM). This model gives unreal data, that is, it is not applicable for the present polymerization systems.

Table 4. Variation of kinetic and colloidal parameters with type of initiator in miniemulsion polymerization of BuA

Initiator type/[initiator] (mol dm^{-3})	Conv.$_f$ (%)	$R_{pmax} \times 10^4$/conv.$_{Rpmax}$ (mol dm^{-3} s^{-1}/%)	R_{pf} ($\times 10^2$ s^{-1})			d_d (nm)	d_p (nm)		N_d ($\times 10^{-16}$ dm^{-3})	N_p ($\times 10^{-16}$ dm^{-3})		N_p/N_d		$\overline{n}$ (particles)
			$x = 0.4$	$x = 0.5$	$x = 1.0$		(a)	(b)		(a)	(b)	(a)	(b)	
APS/0.044	98.3	9.02/20	0.32	0.43	2.04	120	159	158	11.0	0.9	4.8	0.1	0.4	1.12
AIBN/0.06	82.5	19.48/20	0.61	0.81	3.25	115	115	110	13.0	2.4	11.8	0.2	0.9	0.91
DBP/0.04	83.3	16.05/30	0.58	0.80	4.00	110	104	102	15.0	4.9	15.0	0.3	1.0	0.36
MIM/0.01	70.2	4.02/40	0.25	0.40	4.00	130	100	96	9.0	7.2	18.0	0.8	2.0	0.062

Reaction: 1.5 g BuA (0.78 mol dm^{-3} water), 15 g water, 0.015 g polystyrene.
$R_{pf} = R_{pmax}/[I]^x$.
(a) Conversion at R_{pmax} (conv.$_{Rpmax}$); (b) final conversion (conv.$_f$).

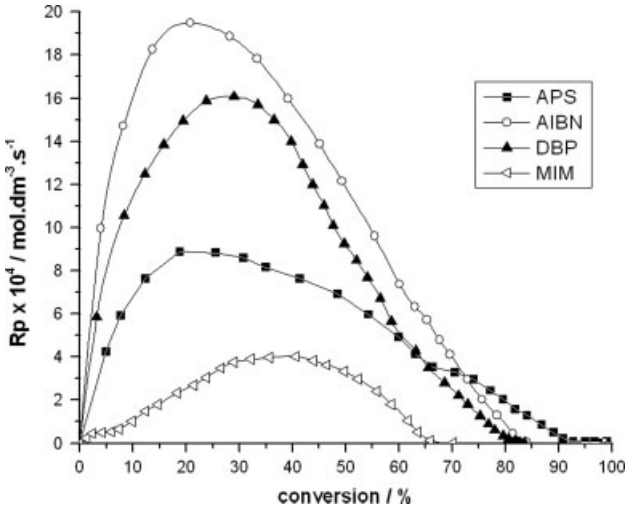

Figure 12. Dependence of polymerization rate on monomer conversion in the miniemulsion polymerization of BuA initiated by various initiators (1.5 g BuA, 15 g water, 0.015 g polystyrene, 0.160 g TW-60, 0.1515 g initiator).

The water-soluble initiators APS and MIM are characterized by the lowest polymerization rates (Fig. 12). The strong deactivation of MIM- and APS-derived radicals in the aqueous phase is expected to be responsible for the lower rate of polymerization. The creation of a network structure by MIM is a further factor that contributes to the decrease in polymerization rate. In contrast, the direct generation of radicals in monomer droplets derived from AIBN and DBP favours both particle nucleation and fast polymerization.

The particle size is known to be proportional to the initiator concentration. Therefore, the largest particles should be formed in the MIM-initiated polymerization and the smallest ones in the AIBN-initiated polymerization. Table 4 shows that the reverse is nearly true. Smallest particles formed by the MIM-initiated polymerization directly confirm the co-emulsifier activity of MIM and/or its grafted oligomers. The highest concentration of polymer particles in the MIM-initiated polymerization should be accompanied by the fastest polymerization. The immobilization of the radicals due to the crosslinking and/or transfer of the reaction loci to the particle surface, however, decrease the rate of polymerization.

Table 4 indicates that the values of N_p/N_d are a function of initiator type. Most of the droplets are nucleated in runs with APS, AIBN and DBP. These data also show that the efficiency of droplet nucleation increases with increasing water solubility of initiator as follows: DBP < AIBN < APS. These data could be attributed to the higher stability of the miniemulsion contributed by the formation of surface-active oligomers formed by the aqueous-phase polymerization of BuA initiated by APS and the chain-transfer events to emulsifier by both APS and AIBN radicals. In both approaches the oligomeric radicals formed are adsorbed at the particle surface and so increase the particle stability. A secondary nucleation observed mainly in runs with MIM (see above) increases the ratio N_p/N_d. Table 1 shows that the addition of MIM decreases the droplet stability. In contrast, addition of poly(ethylene glycol) monomethyl ether (PEOOH) as a co-stabilizer in the inverse miniemulsion polymerization and copolymerization of a water-soluble methacryloyl-terminated PEO resulted in the formation of stable droplets.[40] In the absence of PEOOH, the resulting particles precipitated, indicating poor colloidal stability. The behaviour of MIM in the present study can be attributed to the poor penetration of MIM into the emulsifier shell or the poor co-emulsifier activity of MIM.

Table 4 also shows that the desorption of radicals from the polymer particles is strongest in the MIM-initiated system, that is, the rate-determining process is the desorption of radicals. In contrast, the APS-initiated polymerization is characterized by the highest radical concentration in polymer particles, that is, the desorption of radicals is not important. Also, the desorption of radicals does not influence the polymerization initiated by the partly water-soluble AIBN. The fraction of AIBN in the aqueous phase is responsible for the start of polymerization and the continuous initiation. On the contrary, the polymerization in the DBP-initiated polymerization can start only when the desorption of radicals from the particles (exit from the cage) takes place. The number of radicals per particle for the DBP-initiated polymerization of below 0.5 is in favour of the exit of radicals from particles.

CONCLUSIONS

The miniemulsion polymerization of BuA initiated by a macromonomeric azoinitiator (MIM) and stabilized by a non-ionic emulsifier (TW-60) has been investigated. The rate of polymerization–conversion dependence is described by a curve with a maximum rate at a certain conversion. The polymerization rate increases then decreases with conversion. The increase in the rate of polymerization was discussed in terms of both increased particle concentration and the gel effect. The later decrease in the polymerization rate beyond *ca* 30–50% conversion was attributed to the decrease in monomer concentration at the reaction loci and the immobilization of initiator. The formation of crosslinked nanostructures at medium and high conversion decreases the monomer concentration within the polymer particles and thus the rate of polymerization.

The reaction orders $x = 0.31–0.33$ obtained from the dependence $R_{pmax} \propto [MIM]^x$ favour the emulsion polymerization kinetics more than the solution radical polymerization approach. The increase in the polymerization rate with increasing [MIM] can be attributed to the increased nucleation of polymer particles (or number of reaction loci). The decrease in R_{pmax} above [MIM] = 0.075 g can be discussed in terms of increased contribution of surface particle polymerization and increased desorption of radicals from particles.

The increase in the polymerization rate with increasing [TW-60] can also be attributed to the increased number of polymer particles (number of reaction loci). The contribution of increased density of surfactant layer on the particle surface decreases the entry rate of radicals.

The size of the polymer particles decreases and the number of polymer particles increases with both the TW-60 and MIM concentrations. This behaviour is attributed to the formation of a larger number of smaller monomer and/or polymer particles and a higher particle nucleation rate. This behaviour confirms the co-emulsifier activity of MIM and/or its grafted oligomers. A deviation from this general trend is observed in runs with higher MIM and lower TW-60 concentrations due to crosslinking.

The diameter of the polymer particles slightly decreases while the number of polymer particles increases with increasing monomer conversion. The decrease in the particle diameter with conversion can be discussed in terms of the continuous shrinkage of active monomer/polymer particles which is due to the initiation of polymerization and growth of polymer chains in monomer droplets. The formation of smaller particles with

increasing conversion can also be caused by the partial transfer of monomer from the monomer droplets to active particles (Ostwald ripening). Under such conditions, the particles nucleated at low conversions are larger than those generated at high conversions.

The number of radicals per particle ($\bar{n}$) is much lower than 0.5 which indicates that desorption of radicals from polymer particles takes place. The Ugelstad/O'Toole and Gilbert models suggest an increase in the k'_{des} value with increasing emulsifier concentration (for a run with [MIM] = 0.1515 g) while the Nomura model proposes no variation in k'_{des} with an increasing of both TW-60 and MIM concentrations. The decrease in the k'_{des} values is consistent with the concept that the densely packed emulsifier molecules make a barrier for the entering or exiting radicals. The reverse trend is observed for the k'_{des} values estimated for different emulsifier concentrations at the highest MIM concentration most likely due to the advanced crosslinking or increased immobilization of MIM within the crosslinked polymer particles. The larger amount of emulsifier should increase the number of emulsifier-transferred radicals and their desorption to the continuous phase. A different trend in the k'_{des} values dependent on [MIM] is observed for both Ugelstad/O'Toole and Gilbert models. The former model estimates the increase in the k'_{des} values with increasing [MIM]. The latter model, in contrast, suggests a slight decrease in the k'_{des} values.

The radical entry rate (ρ_a) and the ratio ρ_a/ρ_i increase with increasing MIM concentration. The increase in ρ_a with MIM concentration can be discussed in terms of increased interactions of MIM with the surface of polymer particles which increases the concentration of radicals at the particle surfaces or within the particle shells. The MIM molecules or their graft oligomers can act as surface-active compounds and therefore they are adsorbed at the particle surface which increases both the radical concentration and the colloidal stability of polymer particles. The ratio ρ_a/ρ_i reaches values much above 1.0 which indicates that the emulsion systems obey second-order loss kinetics, that is, the desorbed monomeric radicals will re-enter other particles to either propagate or terminate.

In the case of the use of the different initiators APS, AIBN and DBP, the conversion curve is without a nucleation period. The initiating radicals do not find any barrier in their progress. On the contrary a long nucleation period is observed for the MIM-initiated polymerization and the conversion achieves the lowest value (only 70%) probably due to the creation of a crosslinked structure and the immobilization of MIM chains, that is, the polymerization may proceed under initiator- and monomer-starved conditions.

ACKNOWLEDGEMENTS

This research was supported by VEGA and APVV through grants nos. 2/7013/27, 2/7084/27, −0173-06, −0362-07, −0562-07 and −0030-07. One of the authors (IC) gratefully acknowledges DAAD for financial support.

REFERENCES

1 Hazer B, *Macromol Rep* **A28**:47 (1991).
2 Simionescu I, Comanita E, Pastravanu M and Dumitriu S, *Prog Polym Sci* **12**:1 (1986).
3 Ivanchev SS, *Polym Sci USSR* (Engl transl) **20**:2157 (1979).
4 Yilmaz F, Cianga I, Ito K, Senyo T and Yagci Y, *Macromol Rapid Commun* **24**:316 (2003).
5 Tsukahara Y, Namba S, Iwasa J, Nakano Y, Kaeriyama K and Takahashi M, *Macromolecules* **34**:2624 (2001).
6 Kul D, Yilmaz SS, Ozturk T, Usta A and Misir M, *J Appl Polym Sci* **102**:348 (2006).
7 Hazer B, in *The Polymeric Materials Encyclopedia*, vol. 6, ed. by Salamone JC. CRC Press, New York, pp. 3911–3918 (1996).
8 Hazer B, Synthesis and characterization of block copolymers, in *Handbook of Polymer Science and Technology*, vol. 1, ed. by Cheremisinoff NP. Marcel Dekker, New York, pp. 133–176 (1989).
9 Hazer B, *Makromol Chem* **193**:1081 (1992).
10 Hazer B, Erdem B and Lenz RW, *J Polym Sci A: Polym Chem* **32**:1739 (1994).
11 Savaskan S and Hazer B, *Angew Makromol Chem* **239**:13 (1996).
12 Alli A, Hazer B and Baysal BM, *Eur Polym J* **42**:3024 (2006).
13 Yildiz U, *Macromol Symp* **179**:297 (2002).
14 Tauer K and Yildiz U, *Macromolecules* **23**:8638 (2003).
15 Yildiz U and Hazer B, *Angew Makromol Chem* **265**:16 (1999).
16 Yildiz U and Capek I, *Prog Colloid Polym Sci* **124**:14 (2003).
17 Yildiz U, Landfester K and Antonietti M, *Macromol Chem Phys* **204**:1966 (2003).
18 Asua JM, *Prog Polym Sci* **27**:1283 (2002).
19 Landfester K, Tiarks F, Hentze HP and Antonietti M, *Macromol Chem Phys* **201**:1 (2000).
20 Wang S and Schork FJ, *J Appl Polym Sci* **54**:2157 (1994).
21 Mouran D, Reimers J and Schork FJ, *J Polym Sci A: Polym Chem* **34**:1073 (1996).
22 Tang PL, Sudol ED, Adams ME, El-Aasser MS and Asua JM, *J Appl Polym Sci* **42**:2019 (1991).
23 Alduncin JA, Forcada J and Asua JM, *Macromolecules* **27**:2256 (1994).
24 Chern CS and Chen TJ, *Colloid Polym Sci* **275**:546 (1997).
25 Landfester K, *Macromol Rapid Commun* **22**:896 (2001).
26 Yildiz U, Hazer B and Capek I, *Angew Makromol Chem* **231**:135 (1995).
27 Capek I, *Makromol Chem* **190**:789 (1989).
28 Potisk P and Capek I, *Angew Makromol Chem* **222**:125 (1994).
29 Capek I and Potisk P, *Eur Polym J* **31**:1269 (1995).
30 Reimers J and Schork FJ, *J Appl Polym Sci* **60**:251 (1996).
31 Guo JS, Sudol ED, Vanderhoff JW and Elaasser MS, *J Polym Sci A: Polym Chem* **30**:691 (1992).
32 Harkins WD, *J Am Chem Soc* **69**:1428 (1947).
33 Smith WV and Ewart RH, *J Chem Phys* **6**:592 (1948).
34 Rodiguez R, Barandiaran MJ and Asua JM, *Macromolecules* **40**:5735 (2007).
35 Ferguson CJ, Russell GT and Gilbert RG, *Polymer* **43**:4557 (2002).
36 Yildiz U, Capek I, Berek D, Sarov Y and Rangelow IW, *Polym Int* **56**:364 (2007).
37 Tauer K, Antonietti M, Rosengarten L and Muller H, *Macromol Chem Phys* **199**:897 (1998).
38 Yildiz U and Landfester K, *Polymer* **49**:4930 (2008).
39 Capek I, *Macromol Chem Phys* **195**:1137 (1994).
40 Oh JK, Perineau F and Matyjaszewski K, *Macromolecules* **39**:8003 (2006).

